NMR and Conformational Analysis of Ganglioside GD1a

Subramaniam Sabesan,*,† Jens Ø. Duus,† Tadamichi Fukunaga,† Klaus Bock,‡ and Svend Ludvigsen‡

Contribution No. 5335 from Central Research and Development, Du Pont Company, Wilmington, Delaware 19880-0328, and Department of Chemistry, Carlsberg Laboratory, Gamle Carlsberg Vej 10, Copenhagen, Valby DK 2500, Denmark. *Received October 10, 1990*

Abstract: The hexasaccharide fragment GD1aOS of the glycolipid ganglioside GD1a [αDNeuAc(2-3)βDGal(1-3)-βDGalNAc(1-4){αDNeuAc(2-3)}βDGal(1-4)βDGlc-O-ceramide] was released by ozonolysis followed by mild base treatment and isolated in pure form by ion-exchange chromatography. The compound was analyzed extensively by 500- and 600-MHz NMR spectroscopy. One-dimensional TOCSY and 1D NOESY experiments using Gaussian-shaped pulses as well as 2D NOESY and 2D ROESY measurements were carried out to obtain informations for primary and secondary structural characterizations. These techniques combined with ^{13}C–^{1}H correlation measurements were essential for the complete assignment of hydrogen and carbon chemical shifts. Proton and carbon spin–lattice relaxation time measurements were carried out to probe the dynamic behavior of the hexasaccharide. The interresidual hydrogen distances calculated from the 1D NOESY values were found to be in good accord with the lowest energy model suggested by the HSEA calculations, including those for the glycosidic linkages containing the internal sialic acid residue. Two-dimensional NOESY and ROESY have also been carried out on GD1aOS and the interresidual hydrogen distances calculated from these two methods are remarkably similar. The lowest energy conformer of GD1aOS shows that the internal, branched sialic acid is stacked underneath the GalNAc residue, establishing a hydrogen bond between the carboxylate group of the sialic acid and the acetamido group of the GalNAc unit. Both sialic acid residues are oriented almost perpendicular to the plane of the neutral tetrasaccharide core as the CPK models indicate.

Introduction

Gangliosides belong to a group of glycosphingolipids and are characterized by the presence of one or more acidic sugar units known as sialic acid.[1] They are distributed on the plasma membranes of most vertebrates and are especially enriched in brain and nervous tissues. These glycolipids are believed to be involved in cell–cell adhesion,[2] recognition,[3] and differentiation[4,5] and as receptors for hormones,[6,7] interferons,[8] toxins,[9-12] viruses,[13] and lectins.[14] Gangliosides are known to undergo specific structural changes during oncogenic transformations.[15,16] Investigation of the structure and distribution of these gangliosides from specific tissues has proven to be very valuable in the understanding of their biological roles. In the last few years, attempts have been made to analyze the conformational properties of these complex glycosides to better understand their interactions with receptors.

Gangliosides consist of an oligosaccharide part, which is attached to a lipid known as ceramide.[1] The oligosaccharide part contains a neutral backbone consisting of two to four neutral sugar units [for example, asialo-GM3 βDGal(1-4)βDGlc, asialo-GM2 βDGalNAc(1-4)βDGal(1-4)βDGlc, and asialo-GM1 βDGal(1-3)βDGalNAc(1-4)βDGal(1-4)βDGlc] and the 3-position of the inner galactose is always glycosylated with at least one sialic acid unit. When more than one sialic acids are present, they are also attached to the 3-position of the outer galactose. For example, in ganglioside GD1a which has two sialic acid residues, they are attached to both the inner and the external galactose units of the neutral tetrasaccharide core (asialo-GM1). These oligosaccharides are attached to the ceramide through the glucose residue but can be released by ozonolysis followed by mild base treatment.[17,18] Such a procedure enables the ready dissolution of these complex carbohydrates in aqueous solution and renders them suitable for detailed spectroscopic investigations.

A number of powerful NMR techniques have been developed in recent years for the complete characterization of primary and secondary structures of oligosaccharides.[19-31] Harris and Thornton,[32] Sillerud et al.,[33] and Koerner and co-workers[29,30] have investigated the NMR properties of intact gangliosides and made partial[32] and complete assignments of carbon chemical shifts.[30,32,33] Later Sabesan et al.[18] reported the NMR and conformational properties of the ganglioside known as GM1[βDGal(1-3)-βDGalNAc(1-4){αDNeuAc(2-3)}βDGal(1-4)βDGlc-O-ceramide] and the corresponding free oligosaccharide and presented evidence for the unique conformational properties around the sialosidic

† Du Pont Company.
‡ Carlsberg Laboratory.

(1) Wiegandt, H. In *Glycolipids*; Wiegandt, H., Ed; Elsevier: New York, 1985; New Comprehensive Biochemistry, Vol. 10, p 199.
(2) Cheresh, D. A.; Pierschbacher, M. P.; Herzig, M. A.; Mujoo, K. *J. Cell. Biol.* **1986**, *102*, 688.
(3) Brandley, B. K.; Schnaar, R. L. J. *Leukocyte Biol.* **1986**, *40*, 97.
(4) Edelman, G. M. *Science* **1983**, *219*, 440.
(5) Nojiri, H.; Takaku, F.; Terui, Y.; Miura, Y.; Saito, M. *Proc. Natl. Acad. Sci. U.S.A.* **1986**, *83*, 782.
(6) Mullin, B. R.; Fishman, P. H.; Lee, G.; Ledley, F. D.; Winand, R. J.; Kohn, L. D.; Brady, R. O. *Proc. Natl. Acad. Sci. U.S.A.* **1976**, *73*, 842.
(7) Kohn, L. D. In *Annu. Rep. Med. Chem.* **1977**, *12*, 211.
(8) Besancon, F.; Ankel, H. *Nature* **1974**, *252*, 478.
(9) van Heyningen, W. E.; Carpenter, C. C. J.; Pierce, N. F.; Greenough III, W. B. *J. Infect. Dis.* **1971**, *124*, 415.
(10) King, C. A.; van Heyningen, W. E. *J. Infect. Dis.* **1973**, *127*, 639.
(11) van Heyningen, W. E. *J. Gen. Microbiol.* **1959**, *20*, 301.
(12) Helting, T. B.; Zwisler, O.; Wiegandt, H. *J. Biol. Chem.* **1977**, *252*, 194.
(13) Markwell, M. A. L.; Svennerholm, L.; Paulson, J. C. *Proc. Natl. Acad. Sci. U.S.A.* **1981**, *78*, 5406.
(14) Ravindranath, M. H.; Paulson, J. C.; Irie, R. F. *J. Biol. Chem.* **1988**, *263*, 2079.
(15) (a) Hakomori, S. I.; Kannagi, R. *J. Natl. Cancer Inst.* **1983**, *71*, 231. (b) Singhal, A.; Hakomori, S. I. *BioEssays* **1990**, *12*, 223.
(16) Pukel, C. S.; Lloyd, K. O.; Trabassos, L. R.; Dippold, W. G.; Oettgen, H. F.; Old, L. J. *J. Exp. Med.* **1982**, *155*, 1133.
(17) Wiegandt, H.; Bucking, H. W. *Eur. J. Biochem.* **1970**, *15*, 287.
(18) Sabesan, S.; Bock, K.; Lemieux, R. U. *Can. J. Chem.* **1984**, *62*, 1034.
(19) Hall, L. D.; Morris, G. A.; Sukumar, S. *J. Am. Chem. Soc.* **1980**, *102*, 1745.
(20) Bernstein, M. A.; Hall, L. D. *J. Am. Chem. Soc.* **1982**, *104*, 5553.
(21) Bothner-By, A. A.; Stephens, R. L.; Lee, J. *J. Am. Chem. Soc.* **1984**, *106*, 811.
(22) Lerner, L.; Bax, A. *Carbohydr. Res.* **1987**, *166*, 35.
(23) (a) Homans, S. W.; Dwek, R. A.; Boyd, J.; Soffe, N.; Rademacher, T. W. *Proc. Natl. Acad. Sci. U.S.A.* **1987**, *84*, 1202. (b) Homans, S. W.; Dwek, R. A.; Rademacher, T. W. *Biochemistry* **1987**, *26*, 6553.
(24) (a) Abeygunawardana, C.; Bush, C. A.; Tjoa, S. S.; Fennessey, P. V.; McNeil, M. R. *Carbohydr. Res.* **1989**, *191*, 279. (b) Yan, Z. Y.; Rao, B. N. N.; Bush, C. A. *J. Am. Chem. Soc.* **1987**, *109*, 7663.
(25) Gasa, S.; Nakamura, M.; Makita, A.; Ikura, M.; Hikichi, K. *Eur. J. Biochem.* **1986**, *155*, 603.
(26) Perley, B.; Bossennec, V.; Berthault, P.; Petitou, M. *Tetrahedron Lett.* **1987**, 3331.
(27) Fesik, S. W.; Gampe, R. T., Jr.; Zuiderweg, E. R. P. *J. Am. Chem. Soc.* **1989**, *111*, 770.

0002-7863/91/1513-3236$02.50/0

linkages. It was shown that the aglycon attached to the sialic acid preferred to adopt an antiperiplanar-like orientation to the anomeric carboxylate group (referred to as the anti orientation) and such an orientation enabled an additional interresidual carbohydrate–carbohydrate interaction to further stabilize the conformation. However, it was evident from the study that the sialosidic aglycons that were incapable of establishing similar interresidual stabilizations such as of those in the so-called terminal αDNeuAc(2–3)βDGal fragments (referred as the linear sialosides) also preferred the anti orientation. Recently, two reports have appeared[34,35] which surmised that the conformational properties of sialosides are dependent on whether they are branched or linear. In this paper we report our NMR investigation of oligosaccharide GD1aOS[36a] [Figure 1, αDNeuAc(2–3)βDGal(1–3)βDGalNAc-(1–4){αDNeuAc(2–3)}βDGal(1–4)DGlc-OH] in order to directly compare the conformational properties of the branched and linear sialoside linkages.[36b]

For the complete assignments of hydrogen and carbon chemical shifts, we have carried out 1D TOCSY and 1D NOESY experiments using Gaussian-shaped selective pulses described by Kessler et al.[31] One-dimensional NOESY measurements at several mixing times enabled the construction of NOE build-up curves for anomeric hydrogen and the sialic acid methylene hydrogen signals. These data were used to calculate the interresidual hydrogen distances needed for secondary structural information. We show that these data are in good agreement with the models obtained by the hard-sphere exo-anomeric effect (HSEA) calculations.[37,38]

Experimental Section

αDNeuAc(2–3)βDGal(1–3)βDGalNAc(1–4){αDNeuAc(2–3)}βDGal(1–4)DGlc-OH (GD1aOS). Ganglioside GD1a (30 mg by weight, kindly provided by Dr. L. Cahan and Raju Singh, Division of Neurosurgery, Department of Surgery, UCLA Medical School, Los Angeles, CA 90024) was dissolved in 10 mL of anhydrous methanol. Ozone was gently bubbled through the solution for 30 min followed by dry nitrogen for about 10 min. The ozonide was decomposed by the addition of dimethyl sulfide and the solution was evaporated to dryness. The residue was taken up in methanol–triethylamine (9:1, 20 mL) and left at 4 °C for 5 days. The solution was evaporated to dryness and the residue was extracted successively with chloroform and water (25 mL of each), which were transferred to a separatory funnel. The aqueous layer was separated and washed twice with chloroform (20 mL). The cloudy aqueous layer was filtered through a pad of Celite and the solution was lyophilized. The residue was dissolved in 3 mL of water and applied on a column (1.5 × 9 cm) of Dowex 1X8 resin (phosphate, 200–400 mesh). The column was successively washed with water (125 mL) and 5 mM phosphate buffer (pH 6.8, 175 mL). The product was then eluted with 50 mM phosphate buffer (pH 6.8). The fractions (5 mL each) containing the product GD1aOS[36] as identified by the periodate–resorcinol assay[39] were pooled and lyophilized. The residue was dissolved in 2 mL of deionized water, applied on a column of Sephadex G-15, equilibrated, and eluted with water. Fractions (1.3 mL) were collected and the sialic acid containing fractions were pooled and lyophilized. Weight of the product was 11.7 mg. The identity of the product was firmly established on the basis of ^1H and ^{13}C NMR data (see Figure 2a and Table I).

^1H NMR spectra were recorded on a Bruker AM-600 (600 MHz) or AM-500 (500 MHz) spectrometer equipped with Aspect 3000 computer. Unless specified, all the measurements were done at 295 K. The hydrogen chemical shifts are expressed relative to the HOD signal (4.83 ppm at 295 K), which sets the chemical shifts for acetone at 2.23 ppm. (The chemical shift of the HOD proton signal is temperature sensitive. A standard solution of 5% acetone in D_2O was used for spectral calibration before each measurement and the HOD signal was set relative to the internal acetone signal at 2.23 ppm. Thus at 295 K, the chemical shift of the HOD signal was established as 4.83 ppm. It was also noted that the HOD signal shifted upfield by 0.014 ppm for a 1 K increase in temperature.) Proton spin–lattice relaxation time (T_1) measurements were carried out at 600 MHz by using the inversion-recovery technique. ^{13}C spectra were recorded at 295 K with the GE OMEGA500 instrument operating at 125.74 MHz. The chemical shifts are measured relative to external tetramethylsilane by using the deuterium lock of the spectrometer, which sets the chemical shift of 1,4-dioxane at 66.9 ppm at 295 K.[40,18] Carbon spin–lattice relaxation time (T_1) measurements were carried out with the same instrument by using the inversion-recovery technique and the T_1 values were determined from eight delays (VD = 0.0, 0.01, 0.06, 0.10, 0.16, 0.24, 0.4, and 1.0 s, 1600 transients per delay with 6-s delay between acquisitions) and a fully relaxed spectrum (with 5-s delay time between 180° and 90° pulses, spectral width = 256.5 ppm, pulse width (90°) = 17 μs, data size = 32K points) using a three-point fitting routine. The ^{13}C–^1H correlation experiment was performed at 300 K on a Bruker AM 500 instrument operating at 125.77 MHz for ^{13}C nuclei. Standard Bruker software and the microprogram XHCORRD[41a,b] were used. This procedure, which resulted in the decoupling in the ^1H dimension, was used to obtain increased sensitivity, since the amount of the hexasaccharide available was limited. The 90° pulses for ^{13}C observation and ^1H irradiation were 5.9 and 13.0 μs, respectively. For every t_1 value, 2000 scans were collected and the size of the data matrix was 2048 × 128. These were Fourier transformed in the absolute mode to give a digital resolution of 6.0 and 13.7 Hz/point in the ^{13}C and ^1H dimension, respectively.

One-dimensional TOCSY and 1-D NOESY experiments were performed at 600 MHz. Gaussian-shaped selective pulses were used in these experiments as described by Kessler et al.[31] and the pulses were delivered by the Bruker selective excitation unit. The 70-ms Gaussian pulse (90°) used in these measurements was calibrated as described.[31] For all experiments 16K total data points were acquired with spectral width of 6250 Hz, giving an acquisition time of 1.31 s and a digital resolution of 0.76 Hz/point. The MLEV-17[42] spin-lock pulse sequence was used in the 1-D TOCSY measurements and was delivered by the decoupler at a field strength of 2800 Hz. The sequence was repeated from 2 to 50 times in different experiments giving mixing times from 12 to 290 ms. After the mixing time, a z-filter[43] was inserted with a delay between 90° pulses of 10 ms varied randomly by ±6.6 ms after every phase cycle of 16 scans. This was repeated 16 times giving a total of 256 scans per experiment.

One-dimensional NOESY experiments[31] were performed at several mixing times (10, 100, 200, 400, & 800 ms) and the hard 90° pulse (pulse width 10.9 μs) was delivered by the decoupler. A random variation of ±5 ms was introduced for each mixing time to minimize contributions from zero quantum coherence.[31] Either 256 or 512 transients with a relaxation delay of 2s were collected for each mixing time.

Two-dimensional NOESY experiments were performed at 600 MHz by the method of Bodenhausen et al.[44] using quadrature detection in F_1 by TPPI[45] with the 90° pulse (pulse width 8.5 μs) delivered by the transmitter. Mixing times of 200, 400, and 800 ms were used. Data (2048 t_2 points) were recorded with 24 scans (preceded by two dummy scans) for 512 t_1 values with a spectral width of 3125 Hz in both dimensions. Prior to Fourier transformation, 90° shifted squared sine bell weighting functions and zero filling in both dimensions were applied to give a final data matrix of 2048 × 2048 real points.

Phase-sensitive ROESY[21,46] 2D proton NMR spectra were recorded

(28) Dabrowski, J.; Ejchart, A.; Bruntz, R.; Egge, H. *FEBS Lett.* **1989**, *246*, 229.
(29) Koerner, T. A. W., Jr.; Prestegard, J. H.; Demou, P. C.; Yu, R. K. *Biochemistry* **1983**, *22*, 2676.
(30) Koerner, T. A. W., Jr.; Prestegard, J.; Demou, P. C.; Yu, R. K. *Biochemistry* **1983**, *22*, 2687.
(31) Kessler, H.; Oschkinat, H.; Griesinger, C. *J. Magn. Reson.* **1986**, *70*, 106.
(32) Harris, P. L.; Thornton, E. R. *J. Am. Chem. Soc.* **1978**, *100*, 6738.
(33) Sillerud, L. O.; Yu, R. K.; Schafer, D. E. *Biochemistry* **1982**, *21*, 1260.
(34) Poppe, L.; Dabrowski, J.; Lieth, C. W. V.; Numata, M.; Ogawa, T. *Eur. J. Biochem.* **1989**, *180*, 337.
(35) Breg, J.; Kroon-Batenburg, L. M. J.; Strekcker, G.; Montreuil, J.; Vliegenthart, J. F. G. *Eur. J. Biochem.* **1989**, *178*, 727.
(36) (a) GD1aOS refers to the free oligosaccharide of ganglioside GD1a from which the ceramide portion has been removed. (b) For another recent study on conformations of gangliosides, see: Scarsdale, J. N.; Prestegard, J. H.; Yu, R. K. *Biochemistry* **1990**, *29*, 9843.
(37) Lemieux, R. U.; Bock, K.; Delbaere, L. T. J.; Koto, S.; Rao, V. S. *Can. J. Chem.* **1980**, *58*, 631.
(38) (a) Thogersen, H.; Lemieux, R. U.; Bock, K.; Meyer, B. *Can. J. Chem.* **1982**, *60*, 44. (b) Paulsen, H.; Peters, T.; Sinnwell, V.; Lebuhn, R.; Meyer, B. *Justus Liebigs Ann. Chem.* **1985**, 489.
(39) Jourdian, G. W.; Dean, L.; Roseman, S. *J. Biol. Chem.* **1971**, *246*, 430.
(40) Fransson, L. A.; Huckerby, T. N.; Nieduszynski, I. A. *Biochem. J.* **1978**, *175*, 302.
(41) (a) Bax, A. *J. Magn. Reson.* **1983**, *53*, 517. (b) Ruter, V. *J. Magn. Reson.* **1984**, *58*, 306.
(42) Bax, A.; Davis, D. G. *J. Magn. Reson.* **1985**, *65*, 355.
(43) Sørensen, O. W.; Rance, M.; Ernst, R. R. *J. Magn. Reson.* **1984**, *56*, 527.
(44) Bodenhausen, G.; Kogler, H.; Ernst, R. R. *J. Magn. Reson.* **1984**, *58*, 370.
(45) Marion, D.; Wüthrich, K. *Biochem. Biophys. Res. Commun.* **1983**, *113*, 967.

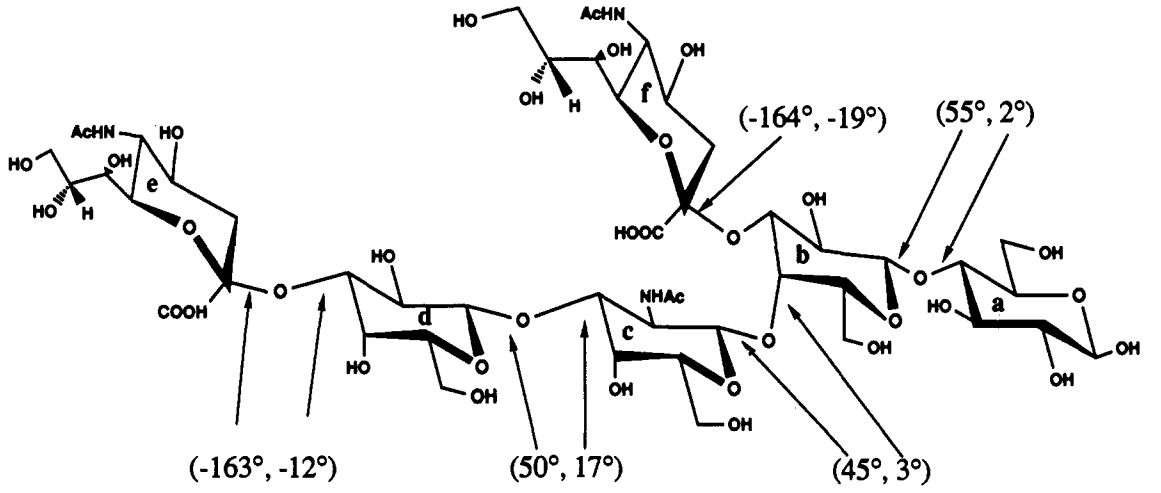

αDNeuAc^{e}(2-3)βDGal^{d}(1-3)βDGalNAc^{c}(1-4)[αDNeuAc^{f}(2-3)]βDGal^{b}(1-4)βDGlc^{a}

Figure 1. Structure of the hexasaccharide GD1aOS. The glycosidic torsion angles corresponding to its global energy minimum as estimated by HSEA calculations are shown in parentheses.

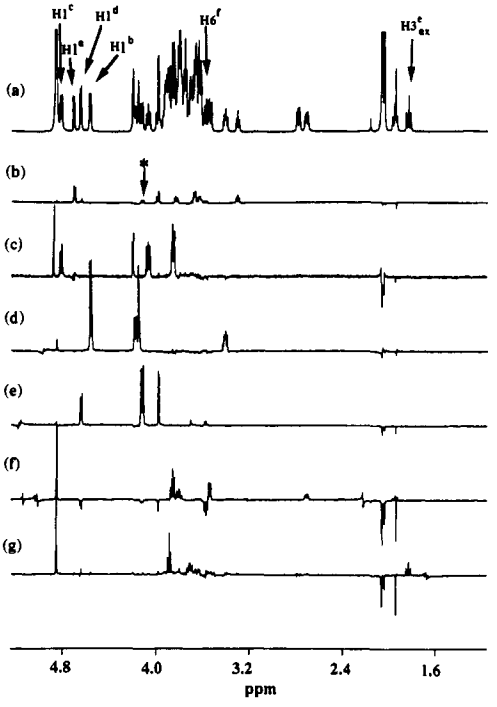

Figure 2. ^{1}H one-dimensional normal (a) and TOCSY (b–g) spectra (290-ms mixing time for TOCSY) of GD1aOS at 600 MHz. These spectra contain from left to right the spin–spin information relay from (b) H-1^{a} to H-6S^{a}, H-6R^{a}, H-3^{a} + H-4^{a}, H-5^{a}, and H-2^{a}; (c) H-1^{c} to H-4^{c}, H-2^{c}, and H-3^{c}; (d) H-1^{b} to H-3^{b}, H-4^{b}, and H-2^{b}; (e) H-1^{d} to H-3^{d}, H-4^{d}, and H-2^{d}; (f) H-6^{f} to H-5^{f}, H-4^{f}, H-3$_{eq}^{f}$, and H-3$_{ax}^{f}$; and (g) H-3$_{eq}^{e}$ to H-5^{e}, H-4^{e}, and H-3$_{ax}^{e}$. The signal indicated by an asterisk is for H-3^{d}, which arises due to partial excitation of signals for H-1^{d}.

on a Bruker AM-500. The spin-lock period in the ROESY experiment was surrounded by two hard pulses as proposed by Griesinger and Ernst[47] to avoid frequency offset dependent effects. All hard pulses were delivered by the transmitter, whereas the spin-lock field came from the decoupler (O1/O2 coherence). The duration of the spin lock was 200 ms at a field strength of 2600 Hz with the lock placed in the middle of the spectrum (3.54 ppm). Quadrature in t_1 was obtained by the hyper complex method of States et al.[48] Data were recorded with 32 scans (preceded by two dummy scans) for 512 t_1 values with a spectral width of 2000 Hz (acquisition time in t_1 = 0.256 s). The acquisition time in t_2 dimension was 0.512 s. The data were transferred to a VAX 11/750 for Fourier transformation. Exponential weighing functions were used for the resolution enhancement of both data sets in both t_1 and t_2 dimensions. The data set was zero filled in the t_1 dimension to produce a final 1024 × 1024 data matrix, which provided a resolution of 1.95 Hz/point.

The HSEA effect calculations were performed following the procedure of Lemieux et al.[37,38a] using the GESA program.[38b] The definition of the torsion angles for the glycosidic linkages are as described in the literature.[37] For neutral sugars shown in Figure 1, the torsion angle ϕ is defined by H-1′–C-1′–O-1′–C-x and ψ is defined by C-1′–O-1′–C-x–H-x. For sialic acids these are defined by ϕ, C-1′–C-2′–O-2′–C-3; ψ, C-2′–O-2′–C-3–H-3.

Results

Ganglioside GD1a is an oligosaccharide αDNeuAc(2–3)-βDGal(1–3)βDGalNAc(1–4){αDNeuAc(2–3)}βDGal(1–4)βDGlc attached to a lipid known as the ceramide as shown in structure 1. The double bond was cleaved by ozonolysis according to the

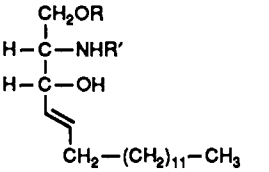

1: R = oligosaccharide; R′ = CO(CH$_2$)$_n$CH$_3$

procedure of Wiegandt and Bucking.[17] Subsequent mild base treatment effected the β elimination, releasing the free hexasaccharide (referred to as GD1aOS and shown in Figure 1) and the lipids. The liberated disialoside selectively adsorbed on an anion-exchange resin, whereas other impurities were eluted out. Subsequent elution with 50 mM phosphate buffer afforded pure hexasaccharide. Structure of the product was confirmed by the proton (see Figure 2a) and carbon NMR spectra as described below.

The sugar units in GD1aOS are denoted by the pyranoside units "a" through "f" starting from the reducing end as shown in Figure

(46) (a) Bax, A.; Davis, D. G. *J. Magn. Reson.* **1985**, *63*, 207. (b) Davis, D. G.; Bax, A. *J. Am. Chem. Soc.* **1985**, *107*, 2820. (c) Breg, J.; Romijn, D.; Vliegenthart, J. F. G. *Carbohydr. Res.* **1988**, *183*, 19.

(47) Griesinger, C.; Ernst, R. R. *J. Magn. Reson.* **1987**, *75*, 261.

(48) States, D. J.; Haberkorn, R. A.; Ruben, D. J. *J. Magn. Reson.* **1982**, *48*, 286.

Table I. ^1H and ^{13}C Chemical Shifts of αDNeuAc^c(2–3)βDGal^d(1–3)βDGalNAc^c(1–4)[αDNeuAc^f(2–3)]βDGal^b(1–4)βDGlc^a (GD1aOS)^a

	αDNeuAc^c		βDGal^d		βDGalNAc^c		αDNeuAc^f		βDGal^b		βDGlc^a	
										^{13}C		
atoms	^1H	^{13}C	^1H	^{13}C	^1H	^{13}C	^1H	^{13}C	^1H		^1H	β α
1		174.3	4.64 (7.7) *[1.46]*	104.8 [0.26]	4.81 (8.4) *[1.46]*	102.8 [0.25]		175.2	4.56 (7.7) *[1.43]*	102.8 [0.25]	α5.25, β4.70 (7.8)	96.0 [0.34] 92.1 [0.27]
2		100.0	3.58 (9.9)	69.4 [0.30]	4.07 (8.4, 11.0)	51.3 [0.24]		101.7	3.41	70.2 [0.23]	β3.31 (8.5)	74.0 [0.34] 71.4 [0.29]
3	1.81 (ax) (12.5) *[0.76]* 2.78 (eq) (4.5) *[0.82]*	39.9 [0.17]	4.13 (9.9, 3.0)	75.7 [0.27]	3.85 (11.0, 3.0)	80.7 [0.21]	1.94 (ax) (12.4) *[1.04]* 2.71 (eq) (4.8) *[1.02]*	37.5 [0.13]	4.19 (9.6 3.0)	74.6 [0.29]^b	3.68	74.6 [0.29]^b 71.6 [0.39]^b
4	3.71 (10.0, 4.6)	68.7 [0.26]	3.98 (3.0)	67.7 [0.21]	4.20 (3.0)	68.0 [0.23]	3.80 (9.9, 4.4)	68.9 [0.23]	4.16 (3.0)	77.1 [0.20]	3.67	78.8 [0.31] 78.8 [0.34]
5	3.89 (10.2)	52.0 [0.27]	3.70 (7.6, 4.6)	74.9 [0.25]	3.77	74.6 [0.25]	3.86	51.9 [0.24]	3.80	74.3 [0.22]	3.63	75.0 [0.31] 70.3 [0.29]
6	3.65	73.1 [0.25]	3.76	61.2 [0.21]	3.80	61.4 [0.17]	3.54 (9.9, 1.5)	73.3 [0.26]	3.84	60.8 [0.15]	3.83 (12.5, 4.9) 3.99 (12.5, <1)	60.4 [0.15] 60.2 [0.14]
			3.76		3.80				3.84			
7	3.62	68.3 [0.24]					3.63 (9.1, 1.5)	68.4 [0.26]				
8	3.93	72.1 [0.29]					3.79	72.5 [0.26]				
9	3.66	62.8 [0.19]					3.65	63.1 [0.17]				
	3.89						3.87					
NH*Ac*	2.04	22.3			2.02	22.9 [0.83]	2.04	22.3				
NH*CO*		175.3 [1.22]				174.3		175.0 [1.07]				

^{a}The hydrogen chemical shifts are expressed relative to HOD (4.83 ppm at 295 K, δ acetone 2.23 ppm) and the carbon chemical shifts are relative to 1,4-dioxane, using the deuterium lock of the spectrometer, which set the chemical shifts for dioxane at 66.9 ppm. The vicinal hydrogen–hydrogen coupling constants in hertzs and the carbon spin–lattice relaxation times (T_1) for the carbon atoms in seconds are shown in the parentheses and brackets, respectively. The values of T_1 reported in this table for the selected hydrogens are italicized in brackets. ^{b}Could not be determined precisely due to overlapped signals.

1. As expected, the glucose unit at the reducing end existed as a 2:1 mixture of β and α anomers exhibiting two sets of hydrogen signals for Glc^a. Since the signals for all the anomeric hydrogens and the C-3 methylene hydrogens of NeuAc residues were well resolved, total correlation spectroscopy (TOCSY) was used to relay spin–spin information from these hydrogens to other hydrogens within a pyranose ring to establish their chemical shift assignment (Figure 2). As noted by Lerner and Bax,[22] the spin–spin information could be relayed in glucose from H-1 to H-6, whereas in galactose it extended only to H-4 from the anomeric hydrogen. To overcome this limitation, 1D NOESY experiments were carried out using Gaussian-shaped pulses to selectively invert the signals belonging to H-4 of galactose. This resulted in NOE's for H-3, H-5, and one of the C-6 methylene hydrogens within the galactose residue. These results were confirmed by 2D NOESY and 2D rotating frame nuclear Overhauser enhancements spectroscopy (ROESY). Once the chemical shifts of the hydrogens were established, most of the carbon resonances could be readily assigned on the basis of the ^{13}C–^1H correlation experiments. Thus, using modern NMR techniques, complete hydrogen and carbon chemical shift assignments could be made for the first time for GD1aOS.

(a) Assignments of ^1H and ^{13}C Chemical Shifts of the Glucose^a Residue. From the set of anomeric hydrogen signals that appear between 4.5 and 5.3 ppm (Figure 2a), the signals for H-1^a of α and β anomers of Glc^a could be readily identified at 5.25 (not shown in the Figure 2a) and 4.70 ppm as they had reduced intensity relative to other anomeric hydrogen signals. These two hydrogens were correlated to the C-1^a signals at 92.1 and 96.0 ppm, respectively, in accord with the published shifts.[49] In 1D TOCSY experiments using Gaussian-shaped selective pulses, the H-1β doublet was selectively excited and spin locked to relay the spin–spin information to all hydrogens in the pyranose backbone (Figure 2b). Starting with a very short spin-lock period, the gradual transfer of spin–spin information to H-2, followed by to H-3 and H-4, and then to H-5 and C-6 methylene hydrogens could be monitored (Figure 2b) and the accurate chemical shifts for these hydrogens could be conclusively established (Table I). It is to be noted that the chemical shifts of H-3 and H-4 were nearly degenerate. Once the chemical shifts of hydrogens were established, the assignments for carbon could be obtained from the ^1H–^{13}C correlated spectrum (Table I). These assignments are found to be in good agreement with the published reports.[18,50]

(b) Assignments of ^1H and ^{13}C Chemical Shifts of the *N*-Acetylgalactosamine^c Residue. Of the remaining three anomeric hydrogen resonances at 4.81, 4.64, and 4.56 ppm, the lowest field signal could be assigned to H-1 of GalNAc^c on the basis of the published data[18,51] on model compounds. This deshielding of H-1^c is consistent with the presence of an adjacent acetamido group. In the 1D TOCSY experiment, spin–spin information transfer from H-1^c to H-2^c (4.07 ppm), H-3^c (3.85 ppm), and H-4^c (4.20 ppm) was clearly seen (Figure 2c). The chemical shift of H-5^c and H-6^c was obtained from both 1D TOCSY and 1D NOESY experiments. In 1D TOCSY experiment, magnetization transfer from the H-4^c signal at 4.20 ppm was seen not only to signals for H-1^c, H-2^c, and H-3^c but also for two more hydrogen signals at 3.76 and 3.80 ppm (H-5^c and H-6^c). In the 1D NOESY, signal enhancements from H-4^c were seen to H-3^c as well as to the above two signals at 3.76 and 3.80 ppm (from the crystal structure of monosaccharides it is known that H-3^c, H-5^c, and H-6^c are within 2.5 Å of H-4^c). The signal at 3.76 ppm also experienced NOE's from H-1^c (Figure 3c) and, thus, it was assigned to H-5^c. The other signal at 3.80 ppm was then assigned to H-6^c. Having assigned the hydrogen chemical shifts, the carbon chemical shifts were obtained from the ^1H–^{13}C correlated spectrum.

(c) Assignments of ^1H and ^{13}C Chemical Shifts of the Galactose^b Residue. Of the remaining two galactose anomeric signals, the doublet at 4.55 ppm (see Figure 2a) could be assigned to H-1^b

(49) Bock, K.; Pedersen, C.; Pedersen, H. *Adv. Carbohydr. Chem. Biochem.* **1983**, *41*, 209.
(50) Sabesan, S. Lemieux, R. U. *Can. J. Chem.* **1984**, *62*, 644.
(51) Sabesan, S. Paulson, J. C. *J. Am. Chem. Soc.* **1986**, *108*, 2068.

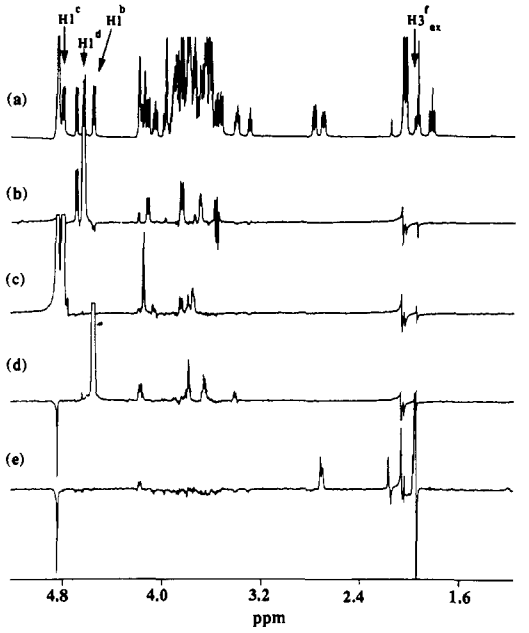

Figure 3. ^1H one-dimensional normal (a) and NOESY spectra at 300 ms (b–e) of GD1aOS at 600 MHz. These spectra contain from left to right the transient NOE's from (b) H-1^d to H-3^d, H-3^c, H-5^d, and H-2^d; (c) H-1^c to H-4^b, H-2^c, H-3^c, H-8^f + H-6^c, and H-5^c; (d) H-1^b to H-3^b, H-5^b, H-3^a + H-4^a, and H-2^b; and (e) H-$3_{ax}{}^f$ to H-3^b and H-$3_{eq}{}^f$.

as it showed a strong NOE to H-4^a across the glycosidic linkage. In the 1D TOCSY experiment (Figure 2d), the spin–spin information transfer from the H-1^b doublet could be seen to signals at 4.19, 4.16, and 3.41 ppm. Of these, the doublet at 4.16 ppm showed a strong NOE to the hydrogen across its glycosidic linkage, namely, H-1^c. This doublet therefore should belong to H-4^b and the remainder of the hydrogens at 3.41 and 4.19 ppm should belong to H-2^b and H-3^b, respectively. The chemical shifts of H-5^b and H-6^b were established by procedures similar to that described above for the GalNAc unit by the 1D NOESY techniques. These hydrogen chemical shifts were then correlated to the carbon network to establish their chemical shifts (Table I).

(d) Assignments of ^1H and ^{13}C Chemical Shifts of the Galactose^d Residue. Finally, the only remaining anomeric hydrogen signal at 4.64 ppm was assigned to H-1^d from which the remaining hydrogen chemical shifts in unit d were established by 1D TOCSY (Figure 2e) and 1D NOESY (Figure 3b) experiments (Table I). The ^{13}C chemical shifts obtained for unit d from the above hydrogen chemical shifts reported in Table I corresponded closely with those published[18] for similar compounds.

(e) Assignments of ^1H and ^{13}C Chemical Shifts of the αDNeuAc^f Residue. The hydrogens at C-3 of the two NeuAc residues provided ideal handles for the 1D TOCSY and NOESY experiments in order to establish the chemical shifts of other hydrogens in the pyranose ring. Of the two triplets observed at 1.81 and 1.94 ppm, the latter could be assigned to H-$3_{ax}{}^f$, as it caused NOE's for the interglycosidic hydrogen H-3^b (see Figure 3e). These signals at 1.94 ppm were coupled to the multiplet at 2.71 ppm, which therefore could be assigned to H-$3_{eq}{}^f$. In the 1D TOCSY experiment, selective excitation of H-$3_{eq}{}^f$ resulted in the spin–spin information transfer to signals at 3.86 (triplet, H-5^f), 3.80 (multiplet, H-4^f), 3.63 (marginal enhancement, H-7^f), and 3.54 ppm (H-6^f). These assignments were further confirmed by selective excitation of H-6^f and observing the spin–spin information transfer to H-5^f, H-4^f, H-$3_{eq}{}^f$ and H-$3_{ax}{}^f$ (Figure 2f). It should be mentioned that the spin–spin information transfer from H-$3_{ax}{}^f$ was not as good as that from H-$3_{eq}{}^f$ and was not useful in chemical shifts assignments. In the 1D and 2D NOESY experiments, NOE's from H-6^f to H-7^f, H-4^f, and H-5^f could be seen and it further confirmed their chemical shifts. From these data, the carbon chemical shifts of C-3 through C-7 were established from the ^1H–^{13}C correlated spectrum. The chemical shifts of the hydrogens at C-8^f and C-9^f were established in the opposite way by first establishing the carbon chemical shifts. The ^{13}C chemical shifts of C-8^f and C-9^f were established to be 72.5 and 63.1 ppm, respectively, by comparing the ^{13}C chemical shifts of GD1aOS with those published for GM1OS.[18] Having done this, the chemical shifts of hydrogens at C-8 and C-9 were established from the ^1H–^{13}C correlated spectrum (see Table I).

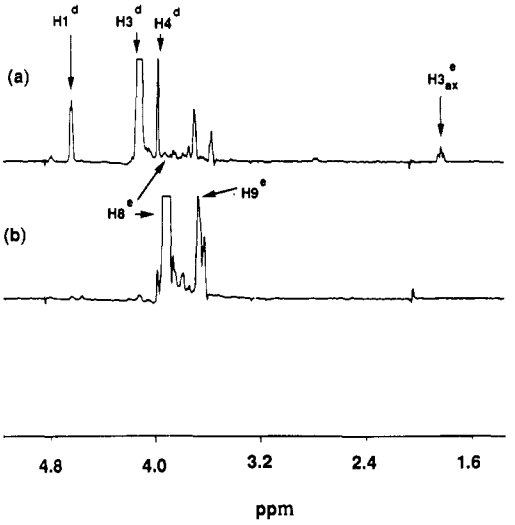

Figure 4. Slices from the 2D NOESY spectra at 400 ms corresponding to the chemical shifts of (a) H-3^d and (b) H-8^e.

(f) Assignments of ^1H and ^{13}C Chemical Shifts of the αDNeuAc^e Residue. Having established the signals for NeuAc^f and all the neutral sugar residues, assignments of hydrogen and carbon chemical shifts for NeuAc^e were much simpler. The resonances for the hydrogens and carbon at the 3-position could be assigned to the signals at 1.81 (H-$3_{ax}{}^3$), 2.78 (H-$3_{aq}{}^e$), and 39.9 ppm (C-3^e). From the 1D TOCSY experiment, the spin–spin information transfer from H-$3_{eq}{}^e$ to H-4^e (3.71 ppm) and H-5^e (3.89 ppm) was clearly seen (Figure 2g). From these, the chemical shifts of the corresponding carbons C-4^e and C-5^e could be established. This then left four unassigned carbons in the ^1H–^{13}C correlated spectrum. These were the signals at 62.8, 68.3, 72.1, and 73.1 ppm. These carbon signals could be assigned to C-9^e, C-7^e, C-8^e, and C-6^e, respectively, on the basis of the published results.[51] These carbon chemical shifts were useful to establish the chemical shifts of H-6^e, H-7^e, H-8^e, and H-9^e. As will be discussed below, the assignment especially for H-8^e was further confirmed by the 2D NOESY experiment, where a cross peak between H-8^e and H-4^d was found (Figure 4b, on the basis of the theoretical models, the distance between these two hydrogens were estimated to be 2.5 Å). A similar NOESY cross peak between H-8^e and H-9^e was seen (Figure 4b) as well. Finally, the chemical shift assignment for C-1^e (174.2 ppm) was made by comparison with the published report.[51]

(g) Hydrogen and Carbon Spin–Lattice Relaxation Times (T_1) of GD1aOS. The T_1's for many of the well-isolated hydrogen signals were measured at both 500 and 600 MHz and as expected they were frequency dependent. The measured values at 600 MHz were 1.4 times longer than those at 500 MHz. Since all NOESY measurements were done at 600 MHz, the proton T_1's at 600 MHz only are reported in the Table I (T_1's are italized in square brackets). In general, the T_1's of all the anomeric hydrogens were nearly the same (1.46 s). Particularly noteworthy were the longer T_1's of the C-3 hydrogens of the internal sialic acid as compared to those of the external one at both 500 and 600 MHz. Carbon T_1 values in the range 0.20–0.27 s were found for the pyranose ring carbon atoms of αDNeuAc^f and the inner sugar residues Gal^b, GalNAc^c, and Gal^d. The T_1 for C-3^f (T_1 = 0.13 s) was shorter than that for C-3^e (T_1 = 0.17 s) and this was opposite of what we observed for the corresponding hydrogen signals. Taken an average value of 0.24 s for the T_1's, the correlation time τ_c for GD1aOS was calculated to be around 0.5 or 2 ns at 500 MHz

Isoenergy Contour Maps

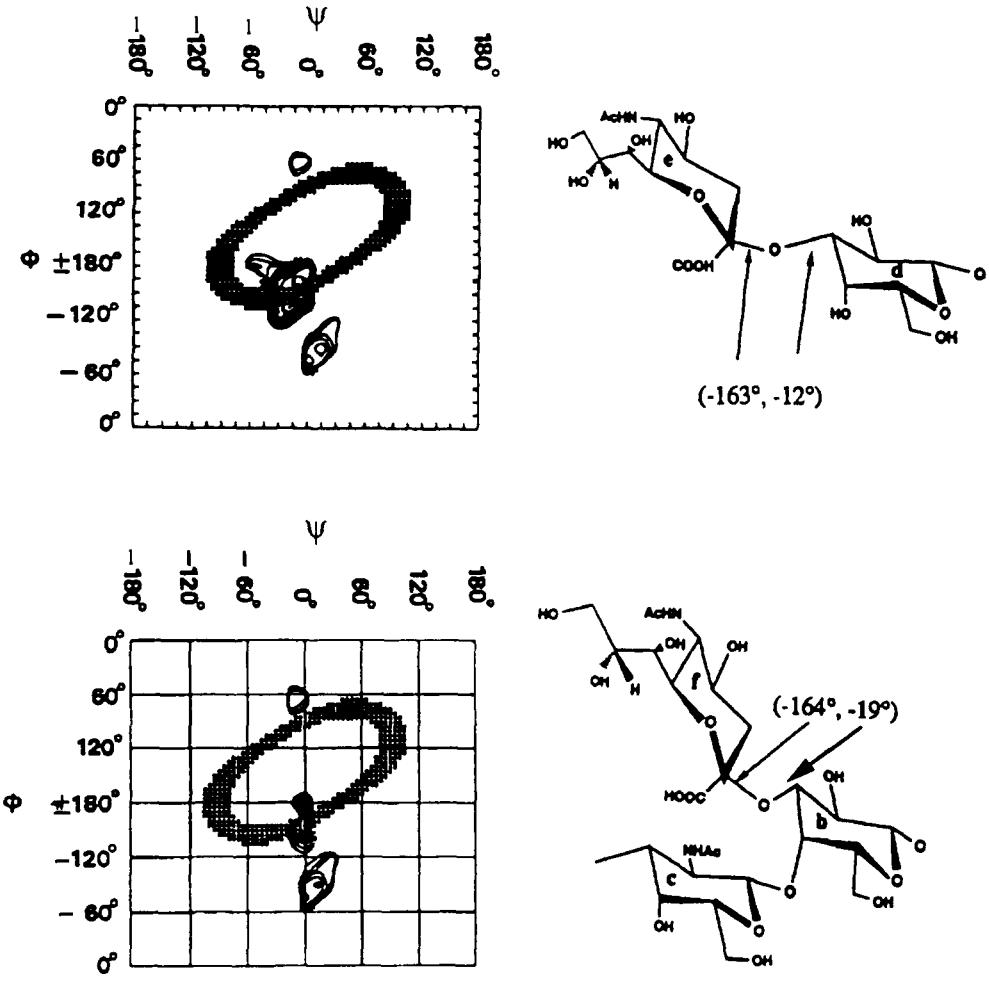

Figure 5. Isoenergy contour maps for the linear (between units e and d) and branched (between units f and b) sialoside linkages. In each case, contour lines represent 1 kcal/mol, and the outside line surrounding each energy well represents conformers 10 kcal/mol above the minimum energy conformer. The shaded ovals represent conformers that have the H-3_{ax} of NeuAc units (e and f) within 2.5 Å from the corresponding aglyconic hydrogens (H-3^d and H-3^b, respectively).

at 295 K by using the expression by Doddrell et al.[52] Theoretical calculation of proton T_1's on the global minimum energy model shown in Figure 1 with a τ_c of 2 ns gave values that were greater than those observed (see Table I) by a factor of 2, whereas the values calculated with τ_c of 0.5 ns gave closer agreement with the observed values. On this basis we conclude that the rotational correlation time of GD1aOS is likely to be around 0.5 ns. As expected for the increased thermal motion of the terminal NeuAc^e and Glc^a, the T_1's for the carbon atoms in these residues are in general slightly longer. However, the differences are not sufficiently large to suggest significantly different segmental motion.

(h) Hard-Sphere Exo-Anomeric Effect (HSEA) Calculations. The HSEA calculation was carried out for the hexasaccharide GD1aOS using the procedure described[18,53] for ganglioside GM1 and linear sialosides. The glycosidic torsion angles calculated for this sialoside at its global energy minimum are shown in Figure 1. The energy contour maps in Figure 5 show various conformers about the sialoside linkages e and f at and within a 10 kcal/mol range from their energy minima. Of the energy wells surrounded by barriers greater than 10 kcal/mol, the one that included the global minimum shared the torsion angles in general agreement with the 1D NOESY, 2D NOESY, and 2D ROESY data discussed below.

For the terminal sialoside linkage between αDNeuAc^e and βDGal^d, rotation of about 20° in the ϕ and ψ torsion angles from the global minimum anti conformation can be accessed within 3 kcal/mol. Other energy minima that are accessible within 10 kcal/mol include a synclinal conformer with glycosidic torsion angles −80°, 10°. It was found that when the terminal sialic acid was placed in the synclinal orientation, the C-9 of the glycerol side chain bumped into the acetamido group of unit c. To relieve this hard interaction, the HSEA calculation changed ψ^c from 17° to −18°, while maintaining the other glycosidic torsion angles constant. This change in ψ^c was smaller (about −14°) if the acetamido group of GalNAc was also relaxed during the course of the energy minimization procedure. Unexpectedly, placement of the glycerol side chain of the sialic acid and the acetamido group in this new orientation resulted in stabilization of about 1 kcal/mol so as to reduce the energy difference between the sialosides in the anti- and this synclinal orientation in GD1aOS to about 2 kcal/mol; the corresponding energy difference for the disaccharide αDNeuAc(2−3)βDGal was estimated to be 3 kcal/mol. Finally, the energy barrier for interconversion between the anti- and the synclinal orientation was estimated to be around 13 kcal/mol, assuming the pyranose rings to be rigid. However, for the branched sialoside containing the residues "f" and "b", the glycosidic linkage was found to be extremely rigid, especially about the torsion angle ψ around the aglyconic carbon C-3^b (Figure 5).

(i) 1D NOESY, 2D NOESY, and 2D ROESY Measurements for GD1aOS. Since many of the hydrogens across the glycosidic

(52) Doddrell, D.; Glushko, V.; Allerhand, A. *J. Chem. Phys.* **1972**, *56*, 3683.

(53) Sabesan, S.; Bock, K.; Paulson, J. C. *Carbohydr. Res.* In press.

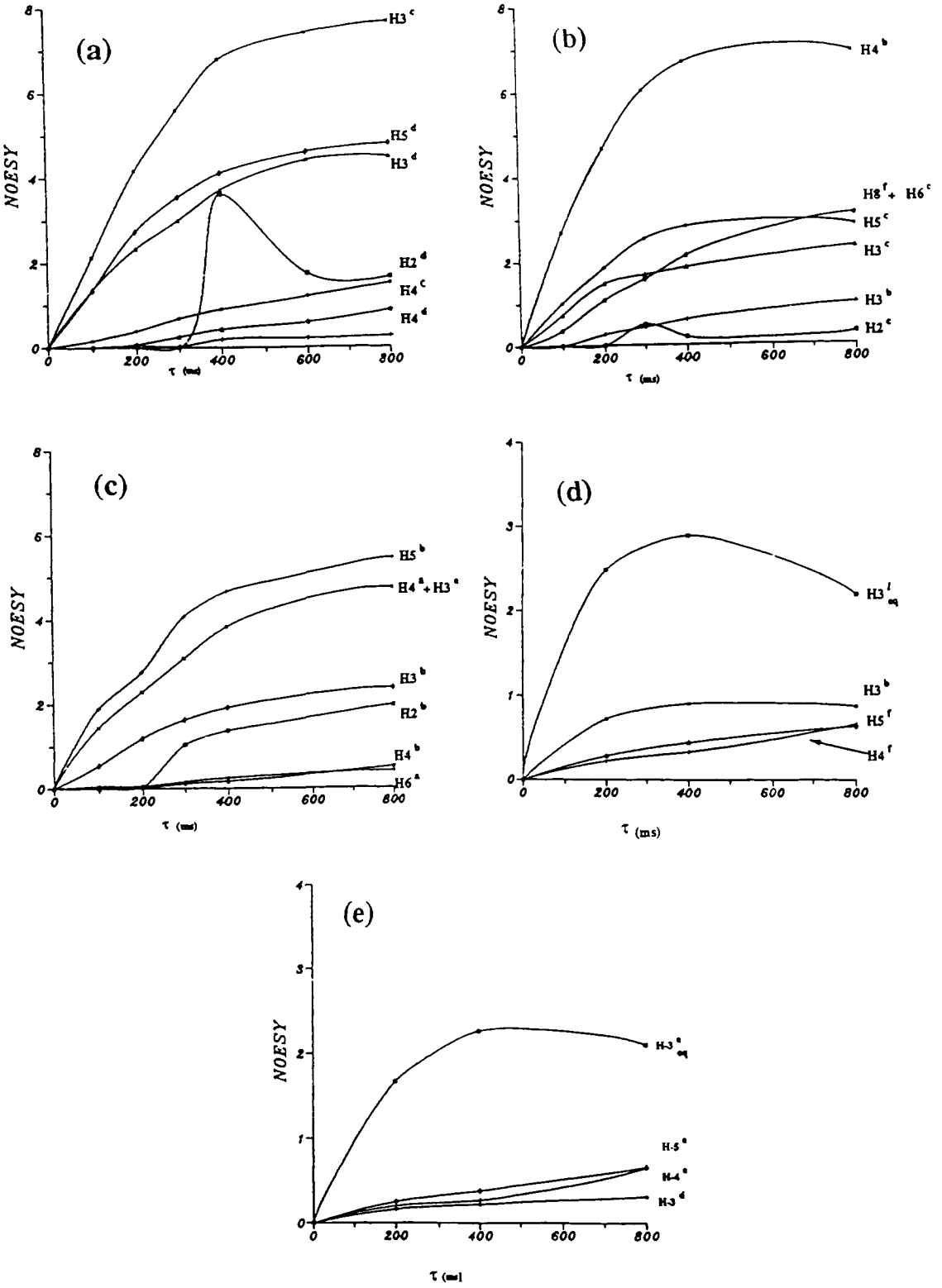

Figure 6. NOE build-up curves for the various hydrogen atoms in units a–f from the anomeric ones (based on transient NOE's obtained from 1D NOESY spectra) and from H-3_{ax}^{e} and H-3_{ax}^{f} (based on NOE's obtained from the 2D NOESY spectra). The selectively inverted hydrogens are (a) H-1^{d}, (b) H-1^{c}, (c) H-1^{b}, (d) H-3_{ax}^{f}, and (e) H-3_{ax}^{e}.

linkages were well separated at 600 MHz. Gaussian-shaped pulses were used to carry out selective 1D NOESY measurements to obtain information regarding the interresidual hydrogen distances. Transient NOE's at mixing times ranging from 100 to 800 ms were measured to ascertain the duration of the linear NOE buildup (Figure 6). The quality of the 1D NOESY information obtained was very good for the glycosidic linkages involving neutral sugar residues and for the internal sialic acid (Figure 3b–e). As can be seen from Table II, for GD1aOS the rate of 1D NOESY buildup was linear below 200 ms (Figure 6) and therefore could be used to calculate interresidual hydrogen distances, assuming the dependence of transient NOE on one spin pair.[54] The interresidual hydrogen distances thus evaluated for those involving anomeric hydrogens and the C-3 hydrogen of the internal sialic

(54) Neuhaus, D.; Williamson, M. *The Nuclear Overhauser Effect In Structural And Conformational Analysis*; VCH Publishers: New York, 1989; p 103.

Table II. Observed NOE's[a] in the 1D NOESY Experiments of GD1aOS for the Intra- and Interresidual Hydrogens from the *Anomeric Hydrogens and H-3$_{ax}$[f] at various Mixing Times*[b]

atom saturated	mixing time (ms)	hydrogens experiencing NOEs						
		H-2[d]	H-3[d]	H-5[d]	H-4[d]	H-2[c]	H-3[c]	H-4[c]
H-1[d]	100		1.36	1.35			2.14	0.16
	200		2.34	2.75	0.08	0.05	4.18	0.39
	300		3.01	3.56	0.25	0.03	5.59	0.69
	400	3.63	3.73	4.12	0.43	0.19	6.78	0.91
	600	1.75	4.42	4.61	0.59	0.21	7.40	1.21
	800	1.67	4.50	4.80	0.88	0.26	7.66	1.52

H-1[d]–H-3[c] dist (Å):[c] H-5[d] internal std, 2.11; H-3[d] internal std, 2.38; av, 2.25; HSEA est dist, 2.46

atom saturated	mixing time (ms)	hydrogens experiencing NOE's					
		H-2[c]	H-3[c]	H-5[c]	H-3[b]	H-4[b]	H-8[f] + H-6[c]
H-1[c]	100		0.73	1.01		2.69	0.36
	200		1.47	1.85	0.26	4.66	1.08
	300	0.49	1.68	2.53	0.42	6.01	1.57
	400	0.19	1.84	2.81	0.60	6.68	2.12
	800	0.29	2.30	2.81	0.97	6.90	3.07

H-1[c]–H-4[b] dist (Å):[c] H-5[c] internal std, 2.05; H-3[c] internal std, 2.09; av, 2.07; HSEA est dist, 2.30

atom saturated	mixing time (ms)	hydrogens experiencing NOE's					
		H-2[b]	H-3[b]	H-4[b]	H-5[b]	H-3+4[a]	H-6[a]
H-1[b]	100		0.54		1.90	1.44	0.05
	200	0.04	1.19	0.02	2.76	2.29	0.06
	300	1.04	1.63	0.11	4.08	3.06	0.16
	400	1.37	1.92	0.17	4.67	3.84	0.25
	800	1.97	2.38	0.51	5.46	4.75	0.40

H-1[b]–H-4[a] dist (Å):[c] H-5[b] internal std, 2.39; H-3[b] internal std, 2.18; av, 2.28; HSEA est dist, 2.42

atom saturated	mixing time (ms)	hydrogens experiencing NOE's		
		H-2[a]	H-3 + 4[a]	H-5[a]
H-1β[a]	100		0.13	0.30
	200	3.49	0.93	1.10
	300	0.33	1.02	1.82
	400	0.60	1.25	2.27
	800	1.15	2.30	3.49

atom saturated	mixing time (ms)	hydrogens experiencing NOE's				
		H-3$_{eq}$[f]	H-5[f]	H-4[f]	H-3[b]	H-3$_{ax}$[f]
H-3$_{ax}$[f] 1D NOESY	100	16.30			1.09	
	200	11.20			1.36	
	300	6.01			2.29	
	400	12.5			2.75	
	800	9.16			1.91	

H-3$_{ax}$[f]–H-3[b,c] dist (Å); H-3$_{eq}$[f] internal std,[c] 2.55; HSEA est dist, 2.02

2D NOESY	200	2.48	0.28	0.22	0.72	13.40
	400	2.89	0.44	0.33	0.90	9.33
	800	2.19	0.63	0.66	0.87	4.48

H-3$_{ax}$[f]–H-3[b,d] dist (Å): H-3$_{eq}$[f] internal std, 2.20; H-5[f] internal std, 2.20; av, 2.20; HSEA est dist, 2.02

atom saturated[b]	mixing time (ms)	hydrogens experiencing NOE's				
		H-3$_{eq}$[e]	H-5[e]	H-4[e]	H-3[d]	H-3$_{ax}$[e]
H-3$_{ax}$[e] 2D NOESY	200	1.67	0.25	0.20	0.16	12.46
	400	2.26	0.38	0.27	0.22	7.92
	800	2.10	0.66	0.65	0.31	3.94

H-3$_{ax}$[e]–H-3[d,d] dist (Å): H-3$_{eq}$[e] internal std, 2.65; H-5[e] internal std, 2.77; av, 2.71; HSEA est dist, 2.11

[a] All the NOE values reported in this table are negative and are expressed as a percentage of the intensity of the inverted hydrogen signals at zero mixing time. [b] Also, the NOE values obtained from the corresponding 2D NOESY subspectra are reported for the H-3$_{ax}$ of sialic acid units e and f. [c] Based on measured NOE's at 100-ms mixing time for intra- and interresidual hydrogens and assuming the NOE dependence to the r^{-6}th distance. [d] Based on the measured NOE ratios at 200-ms mixing time.

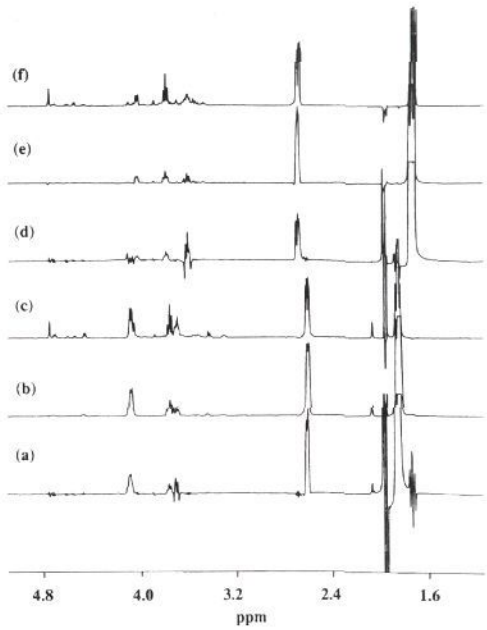

Figure 7. Slices from the 2D NOESY spectra at 200, 400, and 800 ms corresponding to the chemical shifts of H-3$_{ax}$[f] (a–c) and H-3$_{ax}$[e] (d–f), respectively.

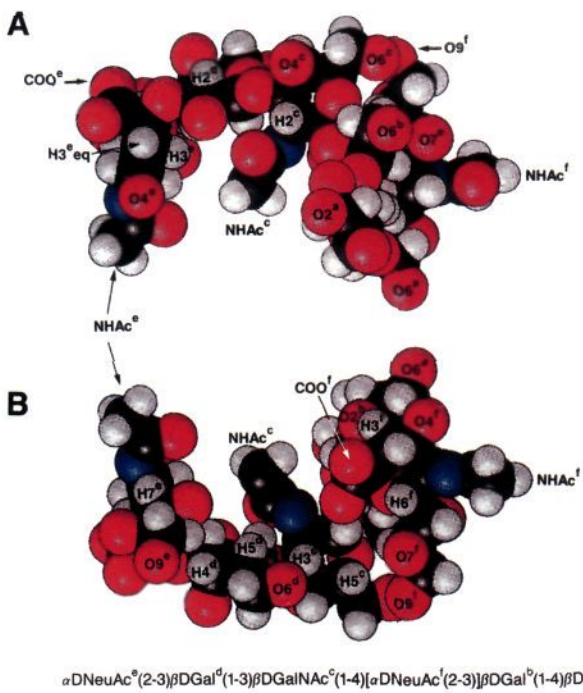

Figure 8. CPK models representing the global minimum energy conformer of the hexasaccharide GD1aOS. Panel A contains the view along the H-2[c]–C-2[c] bond and panel B the view of the molecule from the opposite side.

acid seem to be in good agreement with the distances provided by the HSEA lowest energy model depicted in Figure 1. At greater mixing times contributions other than those from the specific spin-pair cross relaxation appeared to become significant as illustrated in Figure 3 for the 1D NOESY at 300-ms mixing time.

As can be seen from Figure 3b, selective inversion of signals for H-1[d] resulted in very good enhancement of signals for the two intraresidual hydrogens, namely, H-3[d] (4.13 ppm) and H-5[d] (3.70 ppm), and for the interglycosidic hydrogen H-3[c] (3.85 ppm). The

Table III. Internuclear Distances Calculated for the Hydrogen Atoms around the Glycosidic Linkages of the Minimum Energy Conformation Depicted in Figure 1, Experimentally Observed Rotating Frame Enhancement (volume integrals at 200 ms), Cross-Peak Intensities (arbitrary units), and Estimated Internuclear Distances Assuming Linear ROESY Buildup at 200 ms

internuclear dist (Å)									
from H-3_{ax}[e]		from H-1[d]		from H-1[c]		from H-1[b]		from H-3_{ax}[f]	
H-3[d]	2.11	H-3[c]	2.46	H-4[b]	2.30	H-4[a]	2.42	H-3[b]	2.02
ROE	131		311		261[a]		128		430[a]
H-3_{eq}[e]	1.80	H-4[c]	4.00	H-3[b]	4.03	H-3[a]	4.51	H-3_{eq}[f]	1.80
ROE	1112		10		229[a]		*b*		1074
H-4[e]	3.06	H-3[d]	2.57	H-3[c]	2.59	H-3[b]	2.57	H-4[f]	3.05
ROE	101		140		87		93		*b*
H-5[e]	2.58	H-5[d]	2.27	H-5[c]	2.42	H-5[b]	2.28	H-5[f]	2.58
ROE	167		215		241		194		224
H-6[e]	3.96	H-2[d]	3.07	H-2[c]	3.06	H-6A[a]	2.58	H-6[f]	3.96
ROE	73		*c*		*c*		55		44
dist (Å)[d]		$H3_{ax}$[e]–H3[d]		H1[d]–H3[c]		H1[c]–H4[b]		H1[b]–H4[a]	$H3_{ax}$[f]–H3[b]
ROESY		2.68		2.14		2.38		2.44	2.31
NOESY		2.71		2.25		2.07		2.28	2.20

[a] Approximate estimation due to chemical shift overlaps. [b] Could not be determined due to extensive overlap of other hydrogen signals. [c] Zero quantum transition. [d] Based on ROE's for the H-5 of the pyranose unit of the saturated hydrogen as internal standard.

ratios of NOE's at 100 ms for H-3[d]/H-5[d]/H-3[c] was 1:1:1.6 (see Table II). On the basis of the intranuclear hydrogen distances provided by the crystal structure of galactose (H-3–H-1 = 2.56 Å; H-5–H-1 = 2.28 Å), an average internuclear distance between H-1[d] and H-3[c] was calculated to be 2.25 Å. The estimated distance for these two hydrogens based on the HSEA model was 2.46 Å (Table II).

Similarly, enhancements of signals from H-1[c] (Figure 3c) to the two intraresidual hydrogens H-3[c] (3.85 ppm, H-1[c]–H-3[c] = 2.59 Å) and H-5[c] (3.76 ppm, H-1[c]–H-5[c] = 2.42 Å) and to the interresidual hydrogen H-4[b] (4.16 ppm) were observed (Figure 3c). On the basis of the NOE's at 100 ms, the distance between H-1[c]–H-4[b] was calculated to be 2.07, against the HSEA predicted distance of 2.30 Å (Table III). It is to be noted that, in addition to the NOE's mentioned above, a multiplet signal could be seen at 3.79–3.80 ppm (Figure 3c). Examination of the Table I shows that the chemical shifts of both H-8[f] and H-6[e] occur in this region. The 1D NOESY spectrum at 100 ms indicates the signal pattern at 3.79 ppm has the multiplicity expected for H-8[f], while at 200 ms and above overlapped signals from H-6[e] (the NOE is presumably caused indirectly through H-5[e]) were seen. On the basis of HSEA models a strong NOE between H-1[e] and H-8[f] was expected (the distance between them in the lowest energy model was 2.68 Å).

Selective inversion of signals for H-1[b] (Figure 3d) caused NOE's for H-3[b] (4.19 ppm), H-5[b] (3.80 ppm), and the interglycosidic hydrogen H-4[a] (3.67 ppm). On the basis of this observation, the average H-1[b]–H-4[a] distance was calculated to be 2.28 Å, which is to be compared with the HSEA predicted distance of 2.42 Å.

For the internal sialic acid (unit "f"), the 1D NOESY was less successful. For example, selective inversion of H-3_{ax}[f] resulted in the NOE for only one intraresidual hydrogen, namely, H-3_{eq}[f] (at 100–400-ms mixing time). The NOE to H-5[f] was hardly discernible from the noise level. The NOE's to the interresidual hydrogen H-3[b] could be clearly seen (Figure 3e). On the basis of the NOE observed for H-3_{eq}[f], the H-3_{ax}[f]–H-3[b] distance was estimated to be 2.55 Å as shown in Table II.

For the external sialic acid (unit "e") no useful information could be gathered from the 1D NOESY experiments. Two-dimensional NOESY was more useful for this sialosidic linkage. The slices from the 2D NOESY spectra (Figure 7) corresponding to the chemical shifts of H-3_{ax}[f] (Figure 7a–c) and H-3_{ax}[e] (Figure 7d–f) at 300, 400, and 800 ms showed good NOE's from these hydrogens to intraresidual hydrogens H-4, H-5, and H-3_{eq} (units e and f) and to the interresidual hydrogens H-3 of the galactose (units "b" and "d"). The integral of the NOE signals from these slices are reported in Table II. On the basis of the magnitude of NOE's at 200 ms, the average H-3_{ax}[f]–H-3[b] distance was calculated to be 2.20 Å. The distance estimated on the basis of the HSEA model was 2.07 Å. For the external sialic acid, similar calculation based on 2D NOE's provided the H-3_{ax}[e]–H-3[d] distance of 2.71 Å against the HSEA predicted distance of 2.11 Å.

Nuclear Overhauser enhancement measurements in the rotating frame (ROESY) at 500 MHz were also performed to obtain interresidual hydrogen distances and to enable a comparison with those obtained from the NOESY measurements. The ROE values for selected hydrogens of GD1aOS are reported in Table III. The internuclear distances obtained for the hydrogens around the glycosidic linkages from these ROE value at 200 ms mixing time have been compared with the values from NOESY measurements. Within the experimental error, the agreement between these two values is very good.

Bax and Davis[46a] pointed out that the presence of both Hartmann–Hahn (HOHAHA) and ROESY cross peaks is a distinctive disadvantage in ROESY. Breg et al.[46c] also reported that coherent transfer (Hartmann-Hahn cross-peaks) in ROESY spectra resulted in the reduced NOE's. We indeed observed significant effects on a number of intraresidual methine protons, especially on the H-3 hydrogens of the Gal and GalNAc residues from their respective anomeric hydrogen. Fortunately, however, in GD1aOS some of the interresidual NOE's were quite large and the HOHAHA contributions appeared to be either very small or not significant for the intraresidual cross peaks between H-5 and H-3_{ax} of the NeuAc residues (e and f). These HOHAHA effects were not seen between H-5 and H-1 in the galactose[22] (b and d) and GalNAc (c) residues. Thus, using an appropriate intraresidual cross peak (for example, the cross peak between H-5[e] and H-3_{ax}[e]) as the internal standard, we were able to use the volume integrals of the interresidual ROESY cross peaks (for example, the one between H-3[d] and H-3_{ax}[e]) to obtain critical information on the interresidual hydrogen–hydrogen distances (Table III) and the conformation about the glycosidic linkages.

Discussion

The hydrogen and carbon chemical shifts observed for GD1aOS (Table I) were found to be essentially a superposition of the shifts reported[51] for the linear trisaccharide αDNeuAc(2–3)βDGal(1–3)βDGalNAc and the ganglioside GM1[18][βDGal(1–3)-βDGalNAc(1–4){αDNeuAc(2–3)}βDGal(1–4)βDGlc]. However, we were compelled to reverse the earlier chemical shift assignments[18] for C-4[b] and C-3[b] to the resonances at 77.3 and 74.7 ppm, respectively, in accord with the original proposal by Sillerud et al.[33] Crucial to the revised assignment were the resolution and the unambiguous assignment of the signals for H-4[b] and H-3[b]. In the 1D TOCSY spectrum at 600 MHz (see Figure 2d), the two closely spaced resonances, H-4[b] and H-3[b], were resolved and could be unambiguously assigned. This assignment was further confirmed by the observation of transient NOE's between H-4[b] and H-1[c] and between H-3[b] and H-3_{ax}[f] (see Figure 3c,e). Having

done this, the assignments of chemical shifts for C-3^b and C-4^b were deduced by ^{13}C–^1H correlated spectroscopy. In the earlier studies[18] done at 400 MHz, these two hydrogens resonances were essentially degenerate and the carbon assignments were made on the basis of the general principle of glycosidation shifts.[55]

As pointed out by Sillerud et al.[33] and later by Sabesan and Paulson,[51] sialylated oligosaccharides are quite unique in that sialic acids exert only one-half of the expected deshielding to the aglyconic carbon upon sialylation, whereas the shielding effects to the carbons adjacent to the aglyconic carbon are equal or even larger than those normally observed with neutral D-sugars.[55] The situation is even more complex in the branched sialoside linkage (glycosidic linkage f) in GD1aOS, where the effects depend also on the steric crowding around the glycosidic linkage. For example, of the four carbons adjacent to the carbon glycosylated with a NeuAc residue, namely, C-2^d, C-4^d, C-2^b, and C-4^b, the first three carbons are shielded by 1 ppm or more as compared to the corresponding asialo derivative (asialo-GM1).[18] However, the other carbon, C-4^b, experiences an unusual deshielding of about 0.8 ppm. Bock and co-workers[56] attributed the deshielding of this magnitude to the changes in the glycosidic torsion angle around the aglyconic carbon (ψ^b in Figure 1) by about 10° arising from unfavorable interresidual steric interactions. Indeed, the HSEA models predict such unfavorable steric interactions between βDGalNAc^c and αDNeuAc^f in GD1aOS.

The conformational properties of oligosaccharide depend on, among a number of others, two key factors: the stereoelectronic factor known as the exo-anomeric effect and the steric effects around the glycosidic linkages. The HSEA calculations are expected[37,38] to take account of these factors sufficiently. CPK and stereomodels of the minimum-energy conformation of GD1aOS shown in Figures 8 and 9, respectively, were found to be consistent with a number of experimentally determined NMR parameters. Particularly noteworthy in these models depicted in Figures 8 and 9 is the placement of the carboxyl group COO^f within 3.5 Å (see Figure 9) from the acetamido group of GalNAc^c, which enables the establishment of a hydrogen bond between them.[29] Such a hydrogen bond may even force the rotation about the C-1^f–C-2^f bond in such a way as to place one of the carboxyl oxygen atoms closer to the acetamido group. Since both H-6^f and H-4^f bear a syn-diaxial-type relationship to the carboxylate moiety, chemical shifts of these hydrogens should be sensitive to the orientation of the carboxylate group. Indeed, H-6^f is shielded by 0.11 ppm (3.54 ppm, Table I) relative to H-6^e of the external NeuAc^e unit (3.65 ppm), whereas the opposite effect is observed for H-4^f (0.009 ppm deshielded, Table I) relative to H-4^e.

The values for the interresidual hydrogen distances calculated for the neutral sugar residues (Table II) from the 1D NOESY at 100 ms and from the ROESY measurements (Table III) are in good agreement with those expected based on the minimum energy model depicted in Figures 1 and 8. The agreement is remarkably good especially since the lowest energy conformer is certainly not a rigid body and most likely be in equilibrium with other conformers at local energy minima in the NMR time scale. For the branched internal sialic acid (unit f), the strong NOE between H-3$_{ax}^f$ and H-3^b is highly indicative of the close proximity of these hydrogens. Indeed, the isoenergy contour maps (Figure 5) show that the glycosidic linkage between the residues "b" and "f" is quite rigid. Overall, for the conformations of the glycosidic linkages involving units "d", "c", "b", "a", and "f", agreement between the predicted and experimental model is good.

For the sialoside linkage involving the external sialic acid (unit e), the distance between H-3$_{ax}^e$ and H-3^d estimated on the basis of transient NOE (Table II) was much larger (2.71 Å) than that predicted by HSEA calculations (2.11 Å). Thus, conformations other than the anti conformer depicted in Figure 1 appear possible. For example, rapid interconversion between the anti conformer and a synclinal conformer with glycosidic torsion angles (Φ^e, ψ^d = −80°, −10°) is possible. To gauge the contribution of the synclinal conformer relative to the anti,[57] we compared the magnitude of transient NOE from H-3^d to H-3$_{ax}^e$ and H-8^e, and from H-8^e to H-4^d. The HSEA calculations predict that in the anti conformation, the H-3^d–H-3$_{ax}^e$ distance is 2.11 Å, the H-3^d–H-8^e distance is 4.37 Å, and the H-8^e–H-4^d distance is 2.58 Å, whereas in the synclinal conformation, the corresponding distances are 4.15, 2.80, and 4.64 Å, respectively. It can be seen in the 2D NOESY slice corresponding to H-3^d (Figure 4a) that there are strong NOE's from H-3^d in particular to H-1^d, H-4^d, H-5^d, H-2^d, and H-3$_{ax}^e$. Extremely weak and presumably indirect NOE's were also seen for a few other hydrogens such as H-1^c and H-3$_{eq}^f$. A very small NOE is also seen for H-8^e. We could not establish, however, whether this weak enhancement for H-8^e is derived directly from H-3^d or indirectly through H-4^d (the H-8^e–H-4^d distance in the anti conformation is 2.58 Å), as the latter experiences a strong NOE from H-3^d. Similarly, the 2D slice corresponding to the chemical shift of H-8^e shows good enhancement of signals for H-4^d as expected for the anti conformer, in addition to weak enhancements for a number of other hydrogens including H-3^d, H-2^c, H-1^b, and H-1^d. Here again, the direct NOE between H-8^e and H-3^d (expected for synclinal conformation) could not be conclusively established. Even though the NOE data support the anti orientation for the terminal sialoside, the magnitudes of enhancements do not prove its exclusive presence. In the absence of relevant NOE's, we find the establishment of the presence of other conformers, including the synclinal one, difficult.

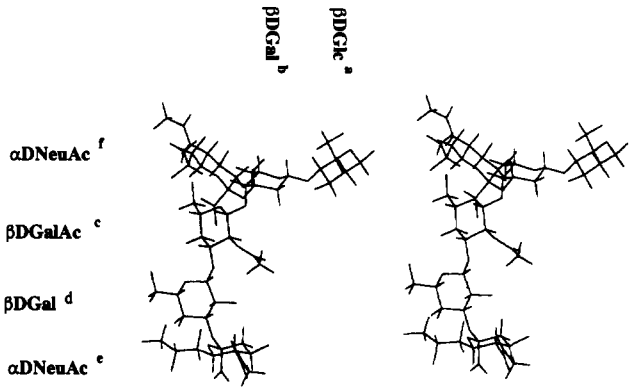

Figure 9. Stereodiagram of GD1a at the global minimum energy conformation depicted in Figure 1.

Poppe et al.[34] recently showed for αDNeuAc(2–3)βDGal-OH there were NOE's from H-3$_{ax}$ of NeuAc to H-3 and H-4 of the galactose (in favor of the anti conformer) and from H-8 of NeuAc to H-3 of the galactose (in favor of the synclinal conformer). The 2D NOESY slices in Figure 4a,b provide no compelling evidence for the presence of appreciable amount of synclinal conformer at least for GD1aOS. HSEA calculation on GD1aOS with the terminal sialic acid placed in the synclinal orientation predicts a hard interaction between the glycerol side chain of the sialic acid unit "e" and the acetamido group of the GalNAc unit "c". To minimize the interaction, the torsion angle ψ^c changed from 17° (as depicted in Figure 1) by about 35° to −18°. The hard interaction was further reduced by relaxing the acetamido group during energy minimization procedures. However, the chemical shifts of atoms in the GalNAc unit are essentially the same in both GD1aOS and GM1, which lacks the terminal sialic acid. This suggests that the changes in ψ^c and the change in the orientation of the acetamido group may occur rapidly on the NMR time scale but cause no significant changes in the chemical shifts.

In conclusion, for GD1a both the HSEA models and experimentally observed NOE's show that the glycosidic linkages involving only neutral sugar residues are associated with torsion angles of about 50° and 0° and place the aglycon O–C synclinal

(55) Bradbury, J. H.; Jenkins, J. A. *Carbohydr. Res.* **1984**, *126*, 125.
(56) Bock, K.; Brignole, A.; Sigurskjold, B. W. *J. Chem. Soc., Perkin Trans. 2* **1986**, 1711.

(57) The anti orientation for sialosides represents the conformers in which the aglycon is placed between the pyranose ring oxygen and the C-3 of the NeuAc unit.

to the anomeric hydrogen. In contrast, the glycosidic torsion angles in the branched sialosides are around -160° and -15°, and the aglycon is placed anti to the anomeric carboxylate substituent. The driving force for the anti orientation is believed to result from the bulky and extensively solvated carboxylate group at the anomeric center, which forces the other bulky substituent aglycon into the least hindered position. This orientation, however, is in accord with the exoanomeric effect. In contrast to the rigidity of the branched sialosides, the terminal sialosides appear to be more flexible. The observed differences between the hydrogen and carbon T_1 values reported in Table I for the branched and linear sialoside residues are in accord with these conclusions. Thus, the experimental results together with the HSEA calculations reported in this paper provide a good structural model for the hexasaccharide of ganglioside GD1a.

Acknowledgment. We express our thanks to Dr. P. J. Domaille for providing valuable assistance in NMR experiments.

Registry No. GD1a, 104443-59-6; GD1aOS, 118701-28-3.

An Electronic Structural Comparison of Copper–Peroxide Complexes of Relevance to Hemocyanin and Tyrosinase Active Sites

Paul K. Ross and Edward I. Solomon*

Contribution from the Department of Chemistry, Stanford University, Stanford, California 94305. *Received August 22, 1990*

Abstract: Self-consistent field-Xα-scattered wave (SCF-Xα-SW) calculations have been performed on a series of copper(II) peroxide structures to evaluate the effects of peroxide bridging geometry on the electronic structure and bonding. The series of structures investigated allows comparison of a set of copper–peroxide monomers and dimers with different binding geometries but with similar ligand environments. The Cu–O and O–O bonding interactions, magnetic exchange interactions, and excited-state transition energies are calculated and compared to experimental properties of structurally related analogues. The primary bonding interaction in all structures involves the in-plane peroxide Π^*_σ orbital bonding with the Cu d ground-state orbitals. The side-on dimer has an additional bonding interaction where the peroxide σ^* orbital acts as a π-acceptor, weakening the O–O bond, consistent with the observed low stretching frequency. The energy difference between the in-plane peroxide Π^*_σ and the out-of plane peroxide Π^*_v orbitals is related to the strength of the copper–peroxide bond and is a measure of the stability of the copper–peroxide adduct. The Π^*_v–Π^*_σ splitting of the side-on dimer is significantly larger than other geometries and is consistent with the observed absorption spectrum. Finally, the electronic structure origin of proposed reaction mechanisms is discussed, and models of relevance to oxyhemocyanin and oxytyrosinase are evaluated.

The ability of copper-containing metalloproteins to reversibly bind and react with dioxygen has been of continued interest in bioinorganic chemistry.[1-5,8] Hemocyanin, tyrosinase, and multicopper oxidases such as laccase, ascorbate oxidase, and ceruloplasmin are examples of metalloproteins that contain copper and interact with dioxygen. Hemocyanin, the oxygen transport protein in arthropods and molluscs, contains a coupled binuclear copper active site which reversibly binds dioxygen as peroxide bridging between the two copper ions.[1] Tyrosinase contains a similar active site and catalyzes the orthohydroxylation of phenols with further oxidation of the catechol product to an *o*-quinone.[1,2] In addition to the coupled binuclear site, the multicopper oxidases also contain additional copper sites. In laccase and ascorbate oxidase there exists a trinuclear copper cluster which is involved in the reduction of dioxygen to water.[3] Understanding the reactivity of these systems requires a detailed knowledge of their electronic structure and that of copper–peroxide complexes in general.

The oxygenated forms of hemocyanin and tyrosinase are the only well-characterized copper–peroxide metalloprotein systems, although oxygen intermediates are known to exist in multicopper oxidases.[4] The active site of oxyhemocyanin contains two tetragonal copper(II) ions separated by 3.6 Å with dioxygen bound as peroxide bridging between the copper ions.[5] Resonance Raman data indicate that the peroxide is symmetrically bound between the copper ions and has a low O–O stretching frequency of 750 cm^{-1}.[6] In addition, oxyhemocyanin is diamagnetic and is not detectable by electron paramagnetic resonance, indicating that the two copper(II) ions are strongly antiferromagnetically coupled ($-2J \geq 550$ cm^{-1} for $H = -2JS_1 \cdot S_2$).[7] Oxyhemocyanin exhibits a unique absorption spectrum with an intense band at 580 nm ($\epsilon \sim 1000$ M^{-1} cm^{-1}) and an extremely intense band at 345 nm ($\epsilon \sim 20000$ M^{-1} cm^{-1}), which have been interpreted as peroxide to Cu(II) charge-transfer transitions of a symmetric bridging peroxide.[5] On the basis of studies of oxyhemocyanin and the met

* Author to whom correspondence should be addressed.

(1) (a) Solomon, E. I.; Penfield, K. W.; Wilcox, D. E. *Struct. Bonding (Berlin)* **1983**, *53*, 1. (b) Solomon, E. I. *Pure Appl. Chem.* **1983**, *55*, 1069–1088. (c) Solomon, E. I. In *Copper Proteins*; Spiro, T. G., Ed.; Wiley: New York, 1981; p 41–108.

(2) Lerch, K. *Met. Ions Biol. Syst.* **1981**, *13*, 143–186.

(3) (a) Spira-Solomon, D. S.; Allendorf, M. D.; Solomon, E. I. *J. Am. Chem. Soc.* **1986**, *108*, 5319–5328. (b) Messerschmidt, A.; Rossi, A.; Ladenstein, R.; Huber, R.; Bolognesi, M.; Gatti, G.; Marchesini, A.; Petruzzelli, R.; Finazzi-Argo, A. *J. Mol. Biol.* **1989**, *206*, 513–529.

(4) (a) Andreasson, L. E.; Branden, R.; Malmstrom, B. G.; Vanngard, T. *FEBS Lett.* **1973**, *32*, 187–189. (b) Andreasson, L. E.; Branden, R.; Reinhammer, B. *Biochim. Biophys. Acta* **1976**, *438*, 370–379. (c) Aasa, R.; Branden, R.; Deinum, J.; Malmstrom, B. G.; Reinhammer, B.; Vanngard, T. *FEBS Lett.* **1976**, *61*, 115–119. (d) Aasa, R.; Branden, R.; Deinum, J.; Malmstrom, B. G.; Reinhammer, B.; Vanngard, T. *Biochem. Biophys. Res. Commun.* **1976**, *70*, 1204–1209. (e) Cole, J. L.; Tan, G. O.; Yang, E. K.; Hodgson, K. O.; Solomon, E. I. *J. Am. Chem. Soc.* **1990**, *112*, 2243–2249.

(5) Eickman, N. C.; Himmelwright, R. S.; Solomon, E. I. *Proc. Natl. Acad. Sci. U.S.A.* **1979**, *76*, 2094–2098.

(6) (a) Larrabee, J. A.; Spiro, T. G. *J. Am. Chem. Soc.* **1980**, *102*, 4217–4223. (b) Freedman, T. B.; Loehr, J. S.; Loehr, T. M. *J. Am. Chem. Soc.* **1976**, *98*, 2809–2815.

(7) Dooley, D. M.; Scott, R. A.; Ellinghaus, J.; Solomon, E. I.; Gray, H. B. *Proc. Natl. Acad. Sci. U.S.A.* **1978**, *75*, 3019–3022.

0002-7863/91/1513-3246$02.50/0